J Appl Electrochem (2009) 39:1259–1265
DOI 10.1007/s10800-009-9793-6

ORIGINAL PAPER

Electrochemical corrosion properties of metal alloys used in orthopaedic implants

Murat Songür · Hüseyin Çelikkan · Faruk Gökmeşe · S. Aykin Şimşek · N. Şükrü Altun · M. Levent Aksu

Received: 28 March 2008 / Accepted: 7 January 2009 / Published online: 29 January 2009

Abstract This study concerns an investigation of the corrosion behavior of 316 stainless steel, CoCrMo and Ti6Al4V alloys in simulated body conditions (ringer lactate) at 37 °C by the use of Tafel plots, mixed potential and electrochemical impedance spectroscopy (EIS). Ti6Al4V alloy has the highest corrosion resistance followed by CoCr alloy. Ti6Al4V–CoCrMO was the best couple for galvanic corrosion with the minimum galvanic potential and current values according to mixed potential theory and Tafel method. It was concluded that Ti6Al4V was the most suitable material for implant applications in the human body.

Keywords Corrosion · Metal alloys · Implant · Galvanic · Impedance

1 Introduction

Numerous metal alloys have been employed as implant materials for the treatment of orthopaedic disorders. Following the evolution of arthroplasty, efforts have particularly focused on the development of more durable implants to serve under high level of duress over many years. Today, the major materials used in implants are 316 stainless steel (ASTM F55-56), Co–Cr alloys (ASTM F75) and Ti6Al4V (ASTM F 136) alloys [1].

Corrosion is a continuous and simultaneous electrochemical process occurring on the surface of metals releasing metal ions and their oxides into the surrounding media. These ions or oxides may be biologically active and potentially carcinogenic [2].

As a result of the rapid wear of polyethylene, metal–metal bearing implants have regained popularity in last two decades, which has made the corrosion properties of these materials increasingly important. These materials have certain advantages and disadvantages when compared to each other. 316 stainless steel is advantageous, as regards its cost effectiveness and durability. However, it is much heavier compared to other materials. Co–Cr alloys have significantly lower corrosion currents. Titanium alloys are relatively lighter and display higher corrosion resistance and passivity in biological media due to the formation of a TiO_2 oxide film on their surface [3].

It is not possible to carry out corrosion tests on these implant materials by the classic weight loss method since their rate of corrosion is extremely small and it takes a long time to obtain practical results. Thus the most popular method in corrosion studies of these materials is the recording of anodic polarization curves by the use of the Tafel method.

The corrosion tests of implant materials may be carried out both in highly corrosive media such as 3.5% (w/w) or 0.9% (w/w) NaCl, 0.1 M HCl or 0.1 M H_2SO_4 and in media simulating biological electrolytes such as Ringer [4, 5], Hank [6, 7] and Tyrode [8] solutions or artificial

M. Songür · S. A. Şimşek · N. Ş. Altun
Department of Orthopaedics and Traumatology, Faculty of Medicine, Gazi University, Ankara, Turkey

H. Çelikkan
Department of Chemistry, Faculty of Art and Sciences, Gazi University, Ankara, Turkey

F. Gökmeşe
Department of Chemistry, Faculty of Art and Sciences, Hitit University, Çorum, Turkey

M. L. Aksu (✉)
Department of Chemistry, Faculty of Education, Gazi University, Ankara, Turkey
e-mail: maksu@gazi.edu.tr

saliva [9] at body temperature of 37 °C as specified in ASTM F 2129.

Clark and Williams [4] carried out corrosion tests of various implant materials in serum albumin and fibrinogen containing electrolytes, representing biological media and found that the corrosion of aluminum and titanium were not affected by such media, while there was a slight increase in the corrosion of chromium and nickel and a significant increase in the corrosion of copper and cobalt. They also observed that the corrosion of molybdenum was significantly inhibited. In another report, Williams stated that the addition of protein to the test solution increased the corrosion rate of stainless steel, but caused no change in the corrosion rate of Ti6Al4V [10]. The fretting corrosion of stainless steel was observed to decrease in protein containing medium and there was no change in the corrosion of pure Ti and its alloys. Hsu et al. investigated the corrosion of Ti6Al4V using phosphate buffered salt (PBS) at different pH values and temperatures [11].

This study concerns the investigation of the corrosion behavior of 316 SS, CoCrMo and Ti6Al4V alloys at a constant temperature of 37 °C in Ringer Lactate solution by the use of Tafel plots and EIS. The compositions of the alloys and of Ringer Lactate solution are given in Tables 1 and 2.

Table 1 Composition of the alloys used in this study

	316 SS	CoCrMo	Ti6Al4V
C	Max. 0.03	0.056	0.015
Si	Max. 1.0	0.41	–
Mn	Max. 2.0	0.54	–
P	Max. 0.025	0.002	–
S	Max. 0.01	0.0016	–
Fe	Remaining	0.29	0.18
Cr	17.0–18.5	27.06	–
Mo	2.7–3.2	5.96	–
Ni	13.5–15.5	0.15	–
Co	–	65.40	–
N	Max. 0.01	0.21	0.007
Al	–	–	5.91
V	–	–	4.13
O	–	–	0.12
Ti	–	–	Remaining

Table 2 The composition of Ringer solution (in 100 mL water)

Sodium lactate (g)	0.31
Calcium chloride (g)	0.02
Sodium chloride (g)	0.6
Potassium chloride (g)	0.03

2 Experimental

The electrochemical measurements were taken using a CH Instruments 660 B Electrochemical Analyser. The working solution was Ringer Lactate solution obtained from Biofarma Inc. (Ankara/Turkey) (Table 2). The temperature was kept constant at 37 °C throughout the study using a Nuve brand thermostat (Ankara/Turkey). Electrochemical measurements were carried out using a three-electrode system. The working electrodes were prepared with the cylindrically shaped alloys embedded in polyester with an exposed surface area of 0.785 cm^2 for 316 SS and Ti6Al4V and 0.503 cm^2 for CoCrMo. The counter and reference electrodes were a 1 cm^2 platinum electrode and Ag/AgCl (3 M KCl), respectively. Prior to use, the electrodes were polished with #500, #700 and #1000 sand paper and 0.5 mm alumina until the surface of the electrode was mirror bright. The system was purged with purified nitrogen to remove dissolved oxygen and blanketed thereafter. The system was subjected to an E-I scan to determine the open circuit potential (OCP) where the magnitude of the current remained constant. The anodic and cathodic Tafel plots were recorded by initiating the potential from 300 mV negative and positive relative to the OCP. Scan rate was 2 mV s^{-1}. The EIS experiments were carried out under the same conditions with which the Tafel plots had been obtained. The lower and upper frequencies of the sinusoidal wave were set at 0.02 and 10^5 Hz. The data obtained were presented as Nyquist diagrams, further interpreted by the impedance simulator Zsimpwin analyzer to determine R_p and C values.

3 Results and discussion

3.1 Anodic polarization diagrams obtained by Tafel method

The resulting plots and data are given in Fig. 1 and in Table 3.

Table 3 shows that the corrosion potential of 316 stainless steel is much more negative than those of CoCrMo and Ti6Al4V alloys. Furthermore the corrosion current of 316 stainless steel is much larger compared to those of CoCrMo and Ti6Al4V alloys. This is an expected outcome, since the corrosion current is directly proportional to the corrosion rate, the lower the corrosion current the better its resistance against corrosion. Similarly, the more positive or anodic the corrosion current, the higher the resistance against corrosion.

By definition, the corrosion of implants implies that a certain amount of ions is released from the implanted metal into the body [12]. The released ions may be deposited in

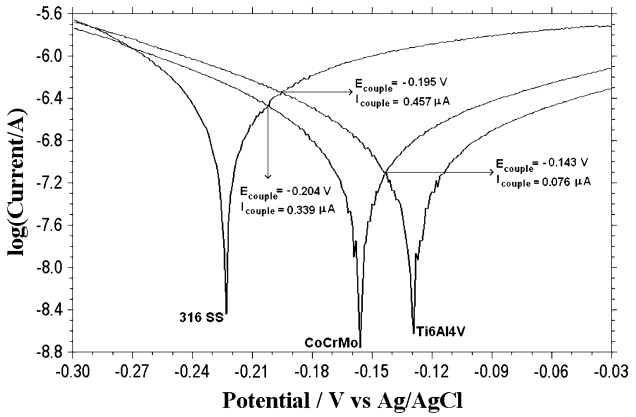

Fig. 1 Tafel anodic polarization results of alloys. **a** 316 SS. **b** CoCrMo. **c** Ti6Al4V

Table 3 Corrosion parameters obtained with Tafel polarization method

	316 SS	CoCrMo	Ti6Al4V
I_{cor} (μA cm^{-2})	0.987	0.230	0.199
E_{cor} (V) vs. Ag/AgCl (3M)	−0.223	−0.156	−0.129

certain parts of the body causing systematic reactions [13, 14]. 316 stainless steel is much more corrosion resistant compared to non-alloyed steels due to the Co, Cr, Mo and Ni it contains and the passive layer formed on its surface.

CoCrMo alloy differs from 316 stainless steel as regards the elements forming the passive layer on its surface. This alloy contains a relatively high amount of molybdenum, which results in a higher degree of surface passivation than Co and Cr. When the corrosion potentials and currents of CoCrMo alloy and 316 SS are compared it can be seen that CoCrMo has a more positive corrosion potential and lower corrosion current. Thus, it can be concluded that CoCrMo alloy is more stabile against corrosion than 316 stainless steel in biological media.

Anodic polarization Tafel plots and the resulting data are shown in Fig. 1 and Table 3. Comparison of Ti6Al4V alloy with CoCrMo alloy showed that the corrosion potential of Ti6Al4V alloy is 27 mV more positive than CoCrMo alloy and its corrosion current is much lower. It can be concluded that Ti6Al4V alloy tends to release less corrosion products into the environment compared to CoCrMo alloy and 316 stainless steel. Both CoCrMo and Ti6Al4V alloys display high resistance against corrosion due to the highly compact passive layers formed on their surface. Regarding Ti6Al4V alloy, besides the formation of highly corrosion resistant TiO_2, oxides of Al and V form an additional passive layer causing further resistance against corrosion. Results of surface analyses with SEM and morphological studies revealed the absence of pitting corrosion on titanium alloys. Consequently these alloys are regarded as the most suitable materials for biomedical applications [15].

When we look at the galvanic corrosion potentials of different alloy combinations the best result is obtained with the Ti6Al4V–CoCrMo couple followed by the Ti6Al4V–316 SS and CoCrMo–316 SS couples. This is another verification that Ti6Al4V alloy is an ideal material for implant purposes (Table 4).

3.2 Results of mixed potential theory

In mixed potential theory the corrosion potential and currents are obtained by extrapolation of anodic and cathodic slopes of the related materials. The graphs are depicted in Figs. 2, 3 and 4.

Ti6Al4V is the most ideal material for implants as indicated by the Tafel method. The passive layer formed upon its surface is responsible for this outstanding corrosion behavior.

3.3 Results of electrochemical impedance

Electrochemical impedance spectroscopy is a versatile technique used in corrosion measurements [16, 17]. The technique is based upon the application of an alternating current starting from low to high frequency at the equilibrium potential of the material. There are EIS studies related to corrosion of Ti6Al4V [11] and Ti5Al4V and Ti6Al4Fe alloys at different pH values in Ringer solution [18].

The EIS diagram of Ti6Al4V alloys is depicted in Fig. 5. Here C_1 and C_2 represent the polarization and double layer capacitances and R_1, R_2 and R_3 are solution, polarization and charge transfer resistances, respectively. The absence of Warburg impedance shows the absence of a

Table 4 Corrosion parameters of alloy couples obtained with the Tafel method and mixed potential theory

Galvanik couples	Corrosion parameters obtained with Tafel method		Corrosion parameters obtained with mixed potential theory	
	E_{couple} (V) vs. Ag/AgCl (3M)	I_{couple} (μA cm^{-2})	E_{couple} (V) vs. Ag/AgCl (3M)	I_{couple} (μA cm^{-2})
Ti–CoCrMo	−0.143	0.076	−0.135	0.132
Ti–316 SS	−0.195	0.457	−0.217	0.617
CoCrMo–316 SS	−0.204	0.339	−0.230	0.550

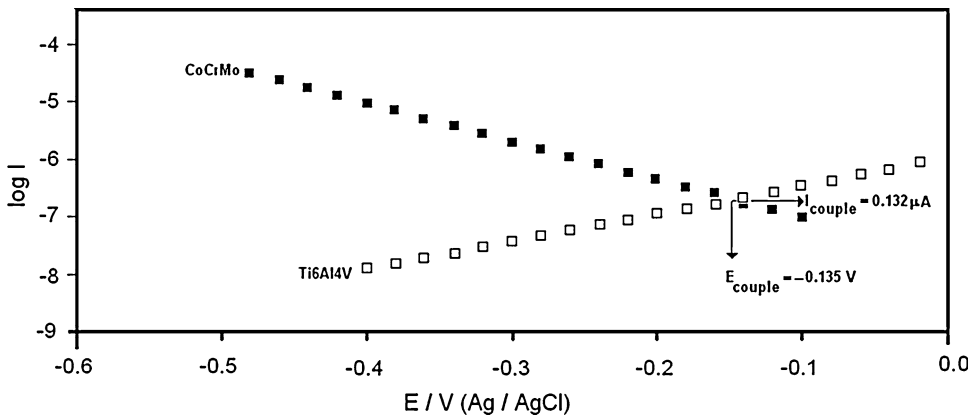

Fig. 2 Corrosion potential and current of Ti6Al4V and CoCrMo alloys obtained with mixed potential theory

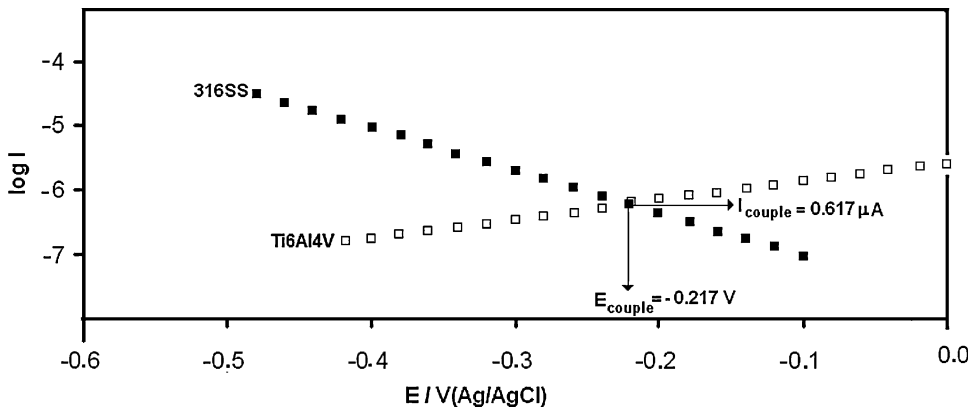

Fig. 3 Corrosion potential and current of Ti6Al4Vand 316 SS alloys obtained with mixed potential theory

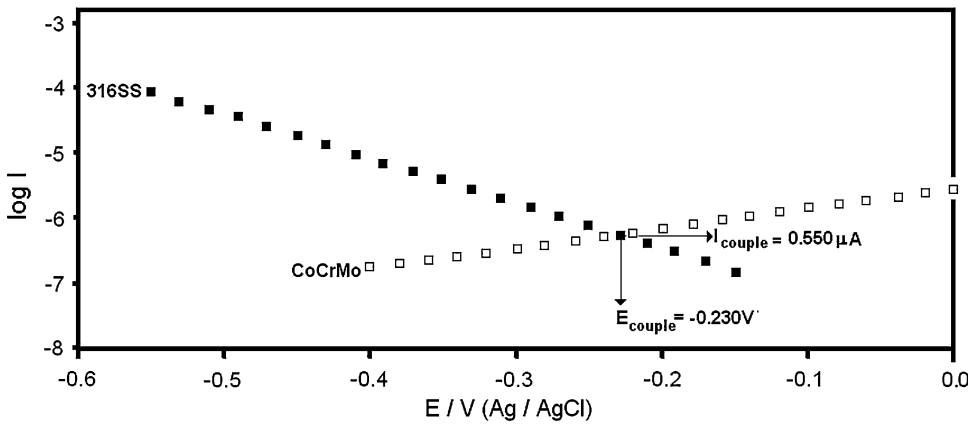

Fig. 4 Corrosion potential and current of CoCrMo and 316 SS alloys obtained with mixed potential theory

diffusion process. The closing appearance of the capacitive loop is an indication that the surface is covered by a two-layered oxide film (generally TiO_2) with a compact inner layer and porous outer layer. The equivalent circuit with two time constants may indicate that the pores were sealed with hydrated material. The outstanding corrosion behavior of the Ti alloy also supports this thesis. Although the polarization resistance (R_2) of CoCrMo alloy is higher, Ti6Al4V alloy is more noble due to its more positive corrosion potential. This may be attributed to better coverage properties of the double layered oxide film formed on the Ti alloy.

Figure 6 is the Nyquist diagram obtained with CoCrMo alloy. The closed nature of the loop gives an equivalent circuit similar to a Randles circuit. Here Q stands for constant the phase element describing the generally non-ideal capacitive behavior of the double layer. The fact that CoCrMo alloy has a higher polarization resistance but

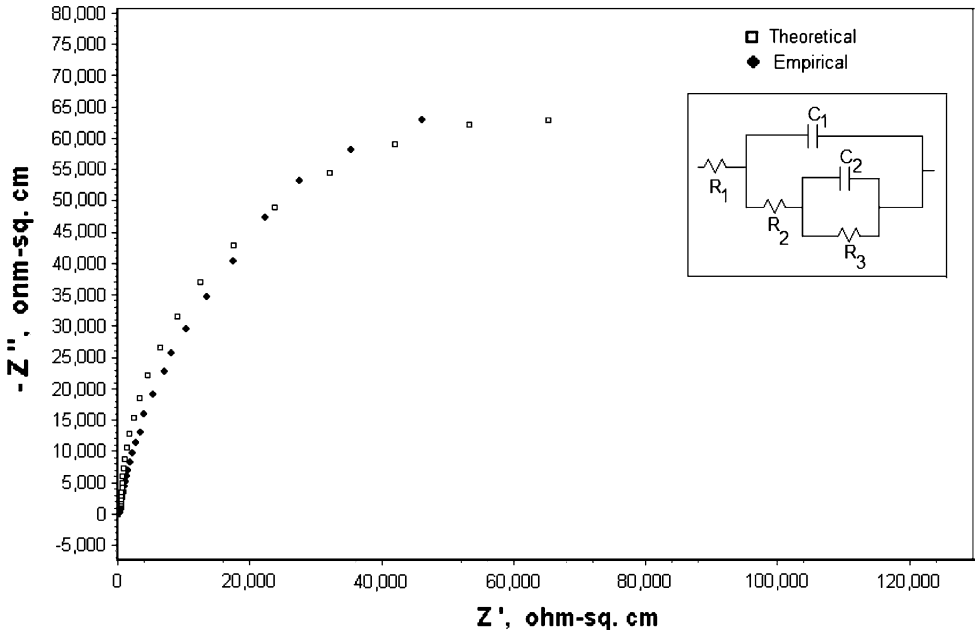

Fig. 5 Nyquist plot of Ti6Al4V alloy. The equivalent circuit is given in *inset*

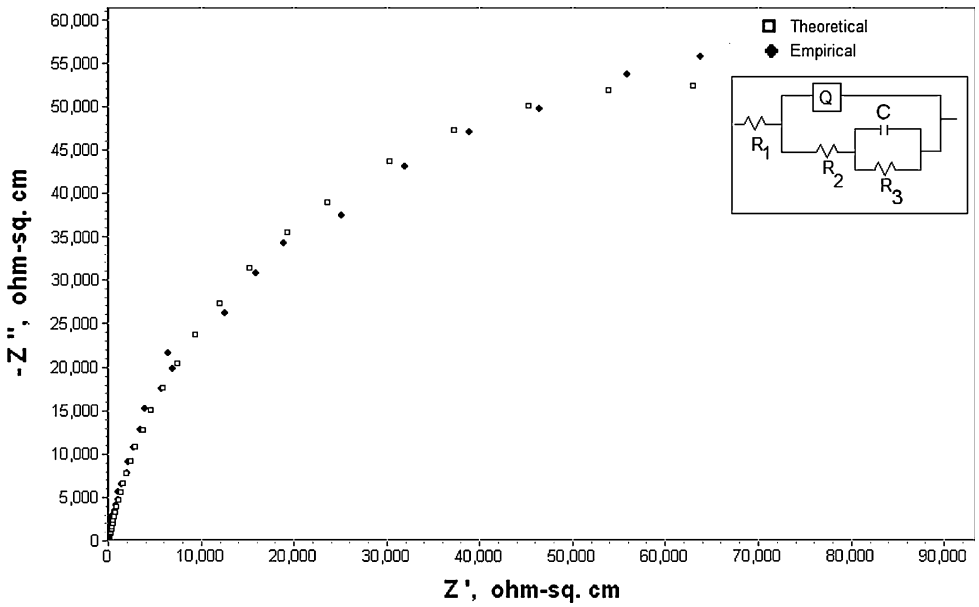

Fig. 6 Nyquist plot of CoCrMo alloy. The equivalent circuit is given in *inset*

more negative corrosion potential can be explained by the nature of the oxide film formed on its surface. This sort of behavior is an indication of the formation of a compact oxide layer. The film is probably much thicker than that formed on the Ti alloy but has inferior coverage properties with higher porosity.

The Nyquist plot of 316 stainless steel (Fig. 7) shows a non-closing capacitive loop with an equivalent circuit with Warburg impedance. This indicates active diffusion controlled dissolution of the oxide layer formed on the surface.

The resulting data obtained from the EIS studies indicates that the highest polarization resistance $R_p(R_2)$ value for the oxide layer formed on any of the alloys is observed for CoCrMo alloy. However Ti alloys give the highest charge transfer resistance $R_{ct}(R_3)$ indicating superior corrosion properties (Table 5).

Figure 8a, b shows the SEM micrographs of clean and oxide covered Ti6Al4V alloy. The corrosion resistant compact TiO_2 layer is formed at −0.05 V which is more positive than its OCP in Ringer Lactate solution. The superior corrosion behavior of Ti6Al4V alloy observed in Tafel and EIS studies was previously attributed to the formation of a TiO_2 layer on its surface. Figure 8b clearly shows the formation of a compact TiO_2 layer on the surface.

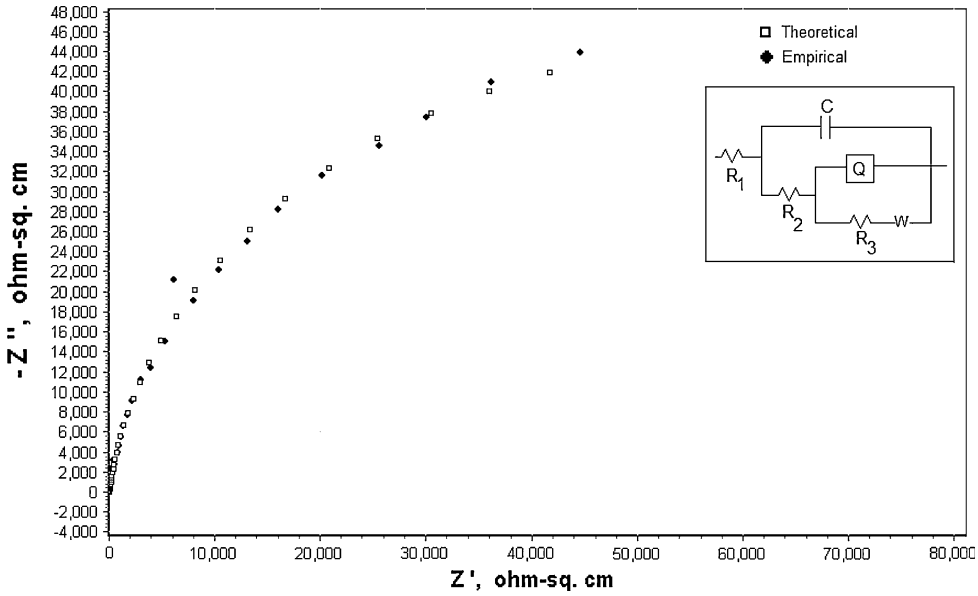

Fig. 7 Nyquist plot of SS316 alloy. The equivalent circuit is given in *inset*

Table 5 EIS data of the alloys investigated

	Ti6Al4V	CoCrMo	316 SS
R_1 (ohm cm^{-2})	1.956	2.418	1.59
R_2 (ohm cm^{-2})	1326	9722	663.1
R_3 (ohm cm^{-2})	1.25×10^5	1.151×10^5	7423.0
C_1 (F cm^{-2})	2.30×10^{-5}	3.358×10^{-5}	4.41×10^{-5}
C_2 (F cm^{-2})	3.58×10^{-5}	–	–
Q_1, Yo (S $s^{1/2}cm^{-2}$)	–	5.42×10^{-5}	3.56×10^{-5}
		$n = 0.8859$	$n = 0.84$
W_1, Yo (S $s^{1/2}cm^{-2}$)	–	–	1.24×10^{-4}

4 Conclusions

Due to its cost effectiveness and availability, stainless steel is a material extensively used for numerous implant applications. However when compared to Titanium and CoCrMo alloys, it has lower corrosion resistance and releases higher amounts of potentially hazardous metal ions, especially nickel, into the body. Ti6Al4V alloy, with its lightness and superior resistance against corrosion, is regarded as the best material for implant applications. It is also far superior with regard to biocompatibility. In addition to titanium alloy, CoCrMo alloy also has a significant corrosion resistance in biological media. Due to its comparable strength and cost effectiveness CoCrMo alloy may also be a good alternative as an implant material.

Acknowledgements The authors are grateful to the Gazi University Research Fund (Project: 04/2003-14) for financial support.

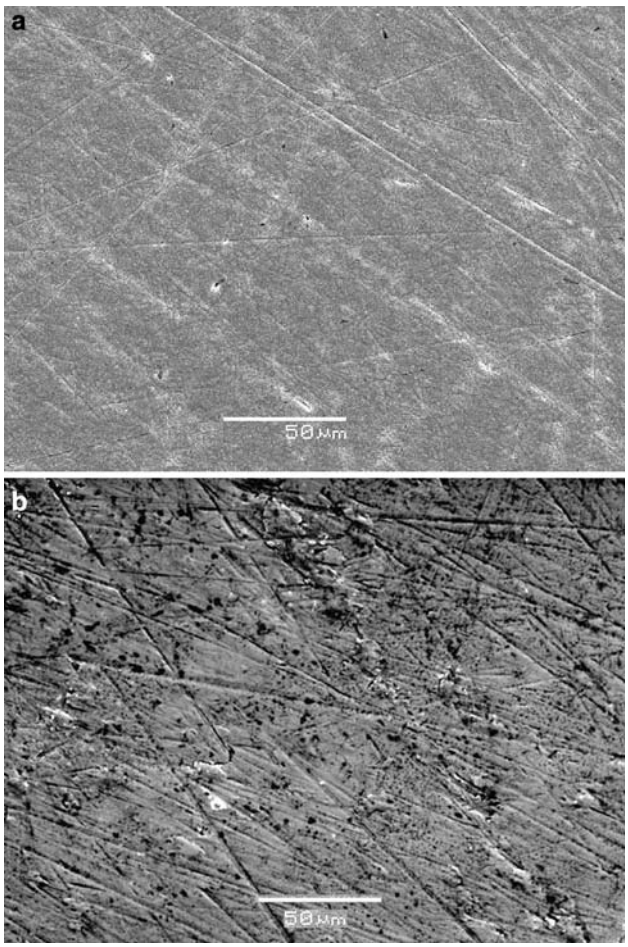

Fig. 8 SEM micrographs of the **a** clean, **b** oxide covered Ti6Al4V alloy surfaces

References

1. Paul JP (1997) J Eng Med 211:119
2. Kazantzis G (1981) Environ Health Perspect 40:143
3. Van Noort R (1987) J Mater Sci 22:3801
4. Clark GC, Williams DF (1982) J Biomed Mater Res 16:125
5. Williams RL, Brown SA, Merritt K (1988) Biomaterials 9:181
6. Bandyopadhya R, Cahoon JR (1977) Corrosion 33:204
7. Gluszek J, Masalki J, Furman P, Nitsch K (1997) Biomaterials 18:789
8. Hoar TP, Mears DC (1966) Proc R Soc Lond A 294:486
9. Milošev I, Metikoš-Huković M, Strehblow HH (2000) Biomaterials 21:2103
10. Reclaru L, Meyer JM (1998) Biomaterials 19:85
11. Hsu RW, Yang C, Huang C, Chen Y (2004) Mater Chem Phys 86269
12. Therin M, Meunier A, Christel P (2003) European Cells and Mater 5:21
13. Gurappa I (2002) Mater Charact 49:73
14. MacDonald D, Mckubre M (1981) Electrochemical impedance techniques in corrosion science: electrochemical corrosion testing. ASTM Spec Tech Publ 727:110
15. Mansfeld M, Kendig M, Tsai S (1982) Corrosion 38:478
16. Popa MV, Demetrescu I, Vasilescu E, Drob P, Lopez AS, Rosca JM, Vasilescua C, Ionita D (2004) Electrochim Acta 49:2113
17. Grosgogeat B, Boinet M, Dalard F, Lissac M (2004) Biomed Mater Eng 14:323
18. Rosca JCM, Santana EDH, Castro JR, Lopez AS, Dro P, Vasilescu C (2005) Mater Corros 56:692